SUPPLEMENTARY INFORMATION

Mechanical coupling maintains the fidelity of NMDA receptor-mediated currents

Rashek Kazi, Jian Dai, Cameron Sweeney, Huan-Xiang Zhou, Lonnie P. Wollmuth

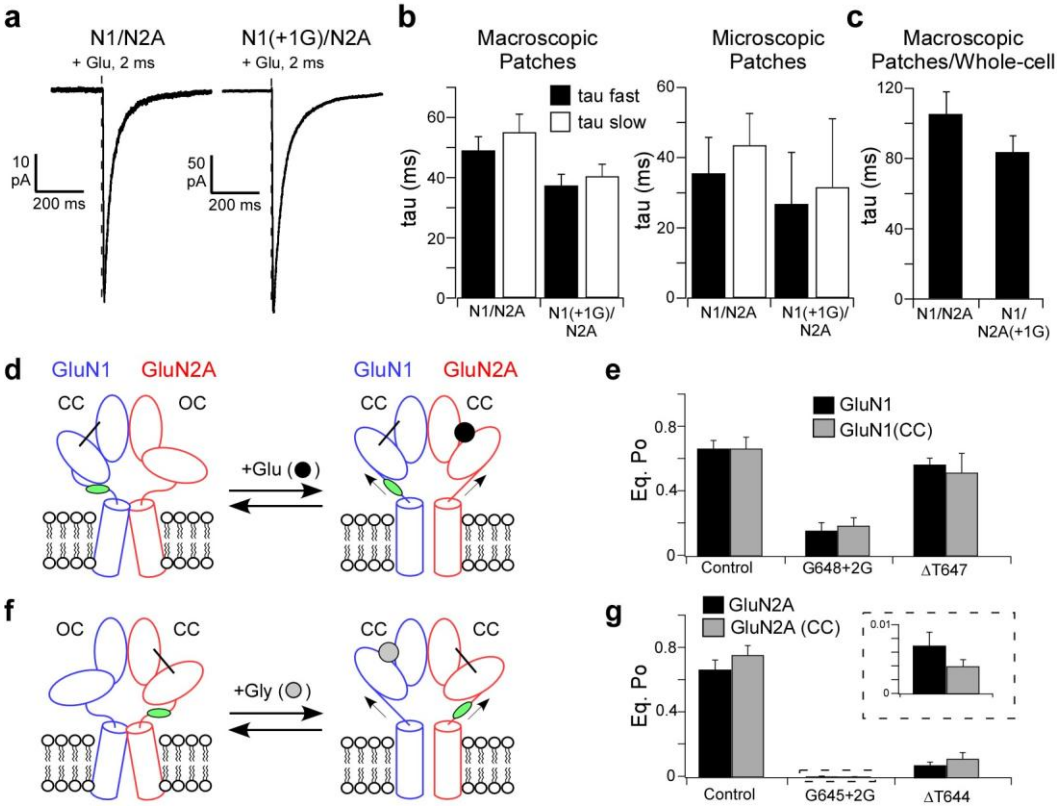

Supplementary Figure 1. Manipulations in the M3-S2 linkers exert effects largely independent of LBD dynamics

(**a–c**) Single glycine insertions in GluN1 or GluN2A have no significant effect on deactivation rates, which for NMDARs are related to ligand unbinding and hence an index of LBD dynamics (Lester & Jahr, 1992, *J. Neuroscience*; Vance et al., 2011, *Nat. Comm*).

(**a**) Representative macroscopic currents from outside-out patches in response to a 2 ms application of glutamate (1 mM). For GluN1/GluN2A(G645+1G), macroscopic currents with 2 ms applications could not be measured but could be using 10 ms applications (not shown).

(**b**) Mean (± SEM, n ≥ 8) rates of deactivation for macroscopic (*left*) and summed currents of microscopic (1–2 channels, from Fig. 1) (*right*) patches for 2 ms applications. Rates were best fit using a biexponential function giving a fast (*black*) and slow (*white*) tau.

(**c**) Mean (± SEM, n ≥ 4) rates of deactivation for outside-out patches/whole cell recordings following a 10 ms application of glutamate for GluN1/GluN2A or GluN1/GluN2A(G645+1G). Rates were best fit with a single exponential function. Deactivation rates in **b** & **c** were not significantly different.

(**d–g**) Forcing the LBD into a closed clamshell configuration has no effect on open probability for M3-S2 insertion or deletion constructs, indicating that manipulations in the M3-S2 linkers do not affect LBD clamshell closure.

(**d & f**) NMDAR LBDs were closed using two engineered cysteines (CC) across the cleft in either GluN1 (**d**) or GluN2A (**f**) (Blanke & VanDongen, 2008, *J. Biol Chem*; Kussius & Popescu, 2010, *J. Neuroscience*). Single-channel activity was recorded in the cell-attached configuration. For GluN1(CC)/GluN2A, the pipette solution contained glutamate (1 mM) with no added glycine. For GluN1/GluN2A(CC), the pipette solution contained glycine (0.1 mM) with no added glutamate.

(**e & g**) Mean (± SEM, n ≥ 3) open probability for the control, +2G, and deletion constructs tested in the wild type LBD (*black*) or CC (*grey*) LBD background. Values for like manipulations in different backgrounds were not statistically different.

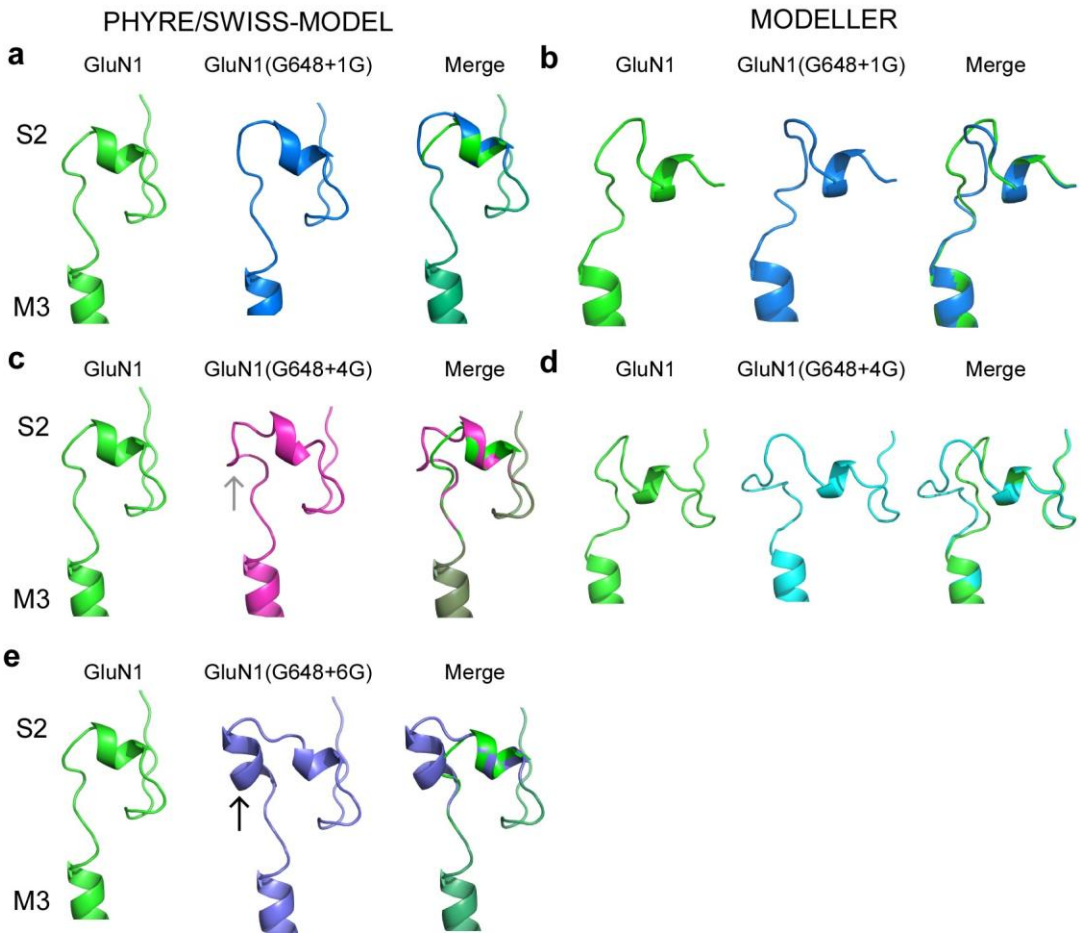

Supplementary Figure 2. Insertions ≤ 4 residues in the GluN1 M3-S2 primarily increase linker length (relates to Fig. 3).

To characterize the structural effects of insertions on secondary structure, we used homology modeling (PHYRE/SWISS-MODEL) (see Online Methods).

(**a–e**) Homology models built using PHYRE/SWISS-MODEL modeling servers (**a,c,e**) or MODELLER (**b,d**) for GluN1(G6458+1G) (**a & b**), GluN1(G648+4G) (**c & d**), and GluN1(G648+6G) (**e**). +1G and +4G insertions predominantly increase the length of M3-S2 while the +6G insertion adds an additional local secondary structure (*black arrow*). The +4G model also shows a potential turn (*grey arrow*).

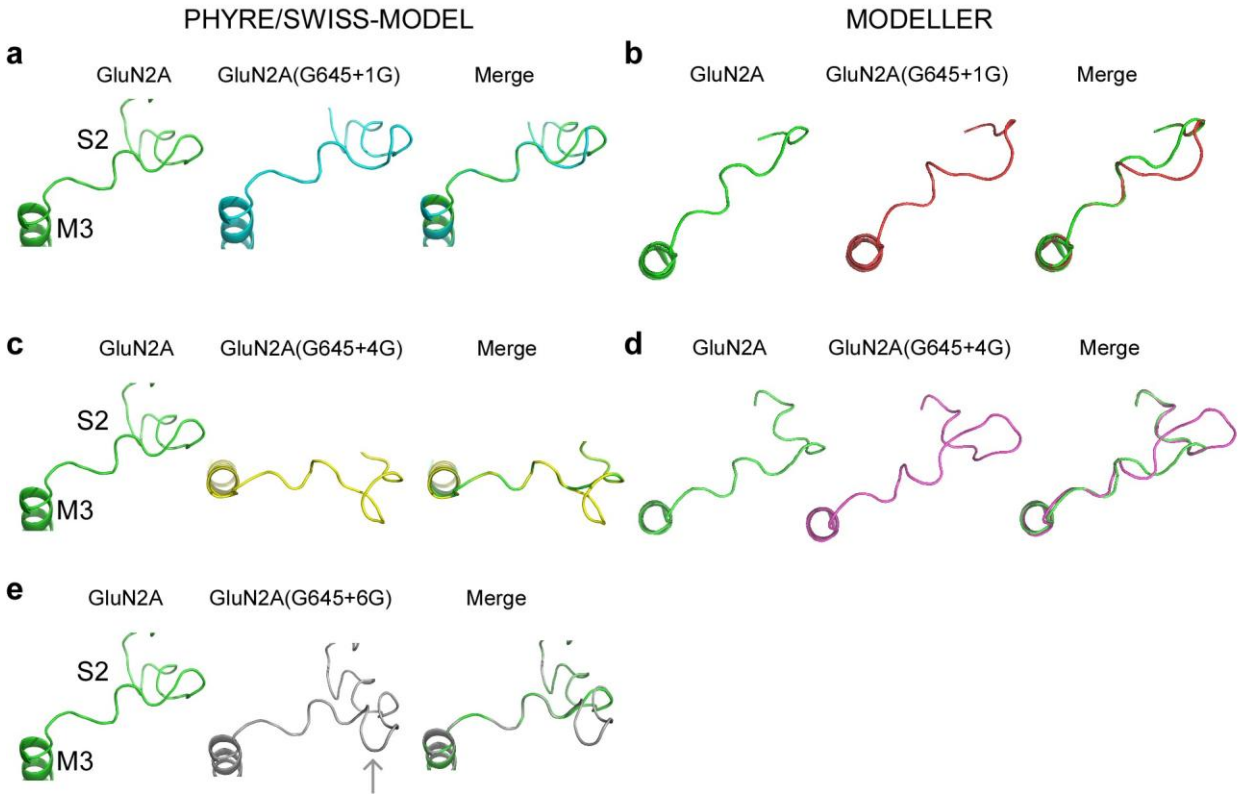

Supplementary Figure 3. Insertions in GluN2A M3-S2 increase linker length (relates to Fig. 3) Same legend as Supplementary Fig. 3 except that modeling is for the GluN2A subunit. None of the insertions produced notable changes in secondary structures though +4G and +6G show a potential turn (*grey arrows*).

Supplementary Table 1. Insertions at different sites in the GluN1 or GluN2A M3-S2 linkers reduce NMDAR pore opening (relates to Fig. 4)

	Total Events	*i* (pA)	P_o	MCT (ms)	MOT (ms)
GluN1/GluN2A	1,565,000 (8)	–7.3 ± 0.4	0.67 ± 0.06	4.3 ± 0.8	9.0 ± 0.9
GluN1					
G648+1G	1,515,000 (8)	–7.6 ± 0.4	0.36 ± 0.06*	10 ± 1.5*	4.9 ± 0.6*
I646+1G	870,000 (5)	–7.3 ± 0.2	0.29 ± 0.03*	7.3± 0.8*	2.7 ± 0.2*^
E644+1G	820,000 (4)	–9.9 ± 0.5*^	0.27 ± 0.05*	9.9 ± 1.4*	3.1 ± 0.4*^
GluN2A					
G645+1G	225,000 (6)	–7.8 ± 0.3	0.08 ± 0.02*	86.8 ± 30*	4.5 ± 0.4*
D641+1G	26,600 (3)	–10.6 ± 1.1	0.01 ± 0.009*^	510 ± 310	2.4 ± 0.5*^
F639+1G	54,000 (3)	–10.2 ± 0.2*^	0.02 ± 0.007*^	260 ± 160	2.3 ± 0.1*^
E637+1G	18,900 (3)	–12.7 ± 0.4*^	0.003 ± 0.001*^	470 ± 140	1.2 ± 0.2*^

Mean values (± SEM) for single-channel current amplitude (*i*), equilibrium open probability (P_o), mean closed time (MCT), and mean open time (MOT). GluN1 and GluN2A subunits containing insertions (bold) were coexpressed with wild type GluN2A and GluN1, respectively. Single-channel recordings were analyzed in QuB (see Online Methods). Number of patches is in parenthesis to the right of total events. P_o is the fractional occupancy of the open states in the MIL fitted single-channel recordings, including long lived closed states. All data was idealized and fit at a dead time of 0.075 ms.

For this and all subsequent Tables and Figures in the Supplementary Information, a significant difference is indicated relative either to GluN1/GluN2A (*); to like manipulations (e.g., single glycine insertions) between subunits [e.g., GluN1(G648+1G)/GluN2A versus GluN1/GluN2A(G645+1G)] ($^{\#}$); or to the single glycine insertions within subunits [e.g., GluN1(G648+1G)/GluN2A versus GluN1(G648+2G)/GluN2A] (^) ($p < 0.05$, two-tailed Student's t-test, unpaired) (see Online Methods).

Supplementary Table 2. Different amino acid insertions reduce open probability (relates to Fig. 4)

	Total Events	*i* (pA)	P_o	MCT (ms)	MOT (ms)
GluN1/GluN2A	1,494,000 (8)	–7.2 ± 0.4	0.67 ± 0.05	5.5 ± 1.0	11.8 ± 1.3
GluN1					
G648+1G	1,260,000 (8)	–7.7 ± 0.4	0.36 ± 0.06*	11 ± 1.7*	5.7 ± 0.7*
G648+1A	580,000 (6)	–8.8 ± 0.2	0.14 ± 0.02*^	22 ± 2.6*^	3.2 ± 0.3*^
G648+1S	310,000 (3)	–7.7 ± 0.6	0.12 ± 0.06*^	34 ± 12	2.9 ± 0.6*^
GluN2A					
G645+1G	225,000 (6)	–7.8 ± 0.3	0.08 ± 0.02*	86.8 ± 30*	4.5 ± 0.4*
G645+1A	16,000 (4)	–7.8 ± 1.1	0.01 ± 0.001*^	630 ± 70*^	3.6 ± 0.3*^
G645+1S	4,700 (3)	–9.1 ± 0.2*	0.01 ± 0.002*^	260 ± 160*^	5.5 ± 0.7*

Table caption is the same as that for Supplementary Table 1 except that the dead time for this analysis was 0.15 ms resulting in a reduced number of events for wild type.

Supplementary Table 3: Additional insertions in the M3-S2 linker further curtail pore opening (relates to Fig. 5)

	Total Events	*i* (pA)	P_o	MCT (ms)	MOT (ms)
GluN1/GluN2A	1,565,000 (8)	–7.3 ± 0.4	0.67 ± 0.06	4.3 ± 0.8	9.0 ± 0.9
GluN1					
G648+1G	1,515,000 (8)	–7.6 ± 0.4	0.36 ± 0.06*	10 ± 1.5*	4.9 ± 0.6*
G648+2G	376,000 (6)	–11 ± 0.8*^	0.14 ± 0.05*^	16.2 ± 4.4*	1.8 ± 0.8*^
G648+4G	472,000 (4)	–12 ± 0.7*^	0.13 ± 0.02*^	15.7 ± 2.3*	2.1 ± 0.1*^
GluN2A					
G645+1G	225,000 (6)	–7.8 ± 0.3	0.08 ± 0.02*	86.8 ± 30*	4.5 ± 0.4*
G645+2G	13,300 (5)	–9.0 ± 1.4	0.008 ± 0.002*^	620 ± 80*^	4.9 ± 1.1
G645+4G	13,700 (6)	–11.3 ± 0.9*^	0.003 ± 0.001*^	3050 ± 860*^	3.6 ± 0.3*

Table caption is the same as that for Supplementary Table 1.

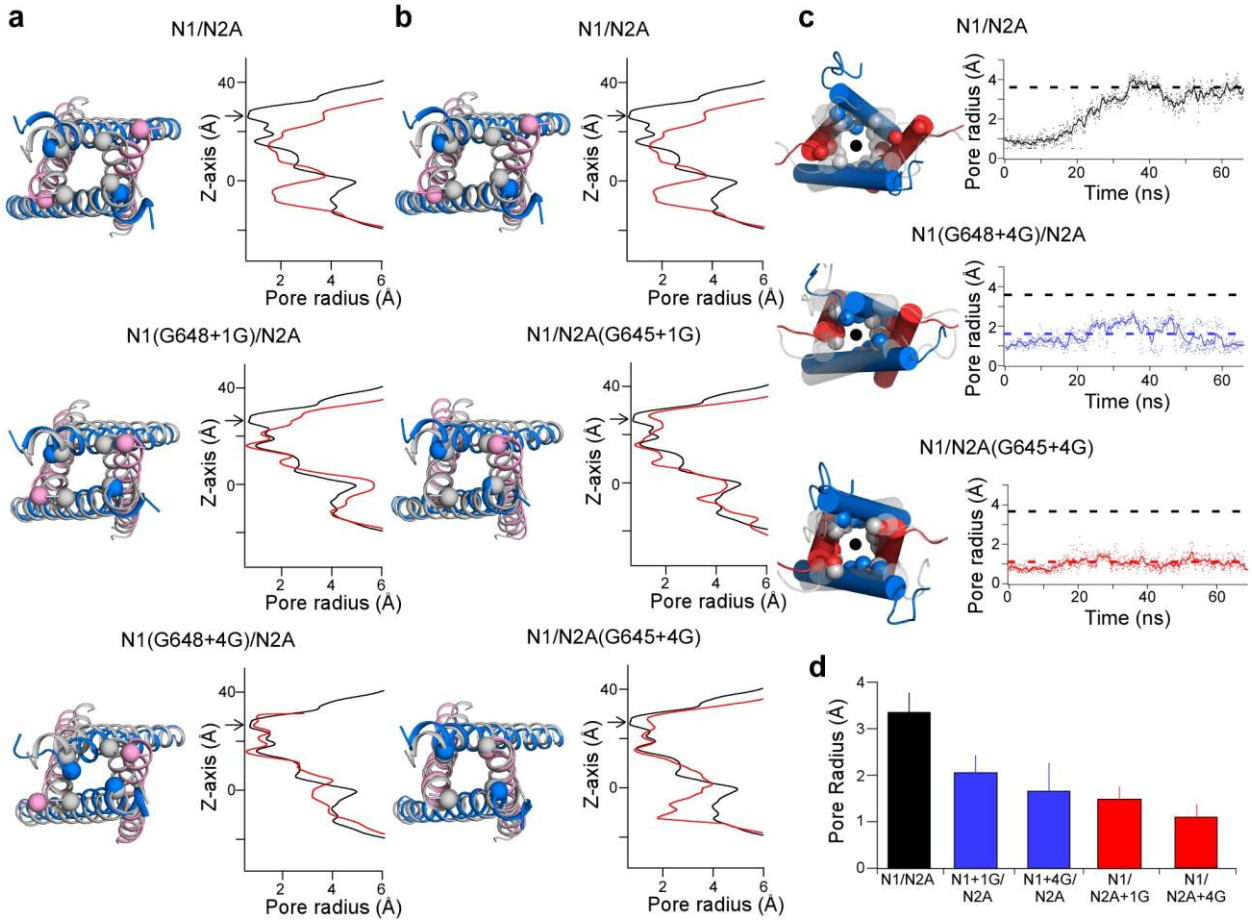

Supplementary Figure 4. M3-S2 insertions reduce the efficiency of pore widening (relates to Figs. 3 & 5)

(**a–b**) M3-S2 insertions reduce pore widening along the length of the pore. *Left*, Top-down view of the pore at the beginning (*grey*) and end (*colored*) of MD simulations for +1G or +4G insertions in GluN1 (**a**, *blue*) or GluN2A (**b**, *pink*). *Right*, Pore radius measurements for representative simulations along the z-axis at the beginning (*black*) and end (*red*) of the simulation. The arrow highlights the outermost ring formed by GluN1(V638) and GluN2A(I635) which was used for pore radius measurements in Figure 3c–e and Supplementary Figures 4c & 4d.

(**c**) Additional insertions in the M3-S2 linker (+4G) further reduce pore widening compared to +1G insertions. *Left*, Overlaid structural snapshots of the ion channel pore (circle) for GluN1(G648+4G)/GluN2A and GluN1/GluN2A(G645+4G) at 0 ns (*grey*, *faded*) and after 65 ns of simulation (*colored*) with spheres highlighting α-carbons of the three gate-forming rings (Fig. 1e). *Right*, Change in pore radius from 0 ns to 65 ns. Shown are the filtered (solid line) and unfiltered (dots) traces for each construct. Pore radius was measured at the outermost ring.

(**d**) Mean (± Standard Deviation) pore radius across the final 700 frames (35 ns) for GluN1/GluN2A (3.3 ± 0.4 Å), GluN1(G648+1G)/GluN2A (2.0 ± 0.4 Å), GluN1(G648+4G)/GluN2A (1.6 ± 0.6 Å), GluN1/GluN2A(G645+1G) (1.5 ± 0.3 Å), and GluN1/GluN2A(G645+4G) (1.1 ± 0.3 Å).

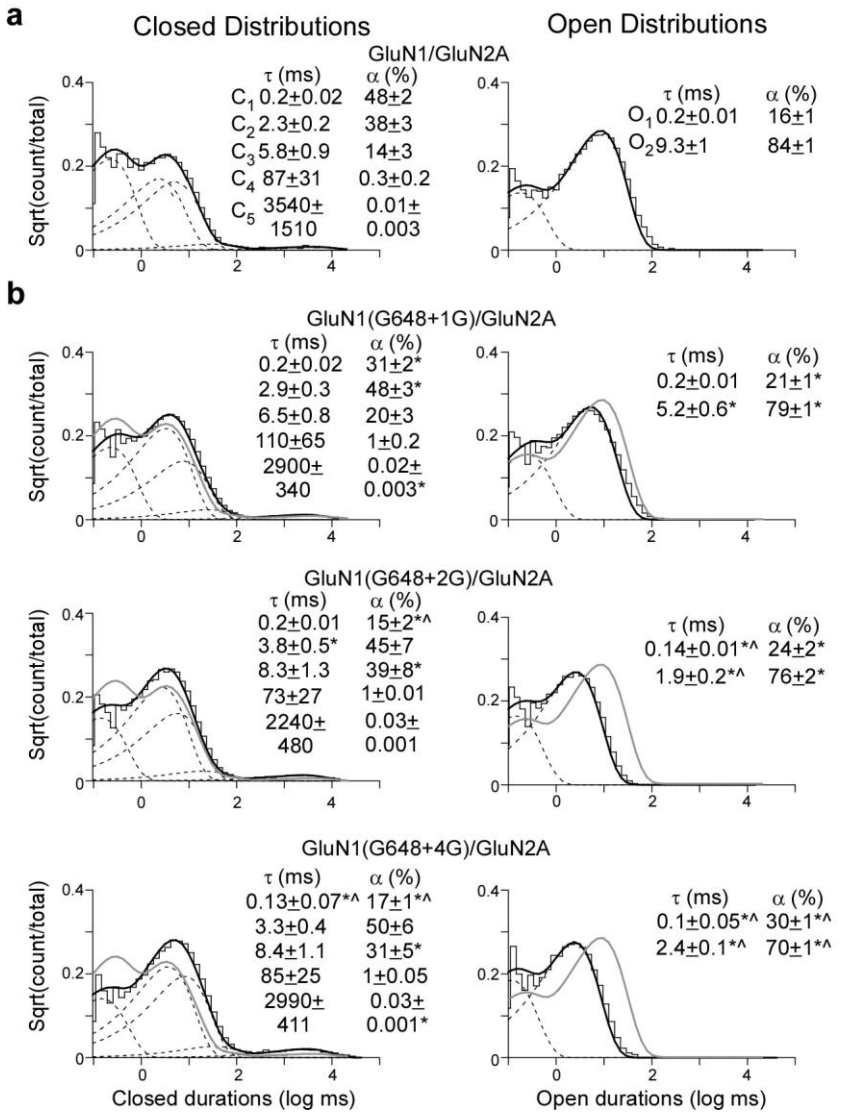

Supplementary Figure 5. Equilibrium open and closed time distributions for wild type and GluN1 insertion constructs (relates to Fig. 6)

Closed (*left*) and open (*right*) durations for GluN1/GluN2A (**a**) and GluN1(G648+nG)/GluN2A (**b**) where n = 1, 2, or 4. For all constructs, the closed-time distributions were best fit by five exponentials. Although there was considerable variation across patches in terms of the number of open state exponentials (2 to 4), we fitted all open state distributions with 2 exponentials to permit comparisons across different constructs. *Insets*, mean values (±SEM) for closed and open state durations (*left*, τ, ms) and occupancies (*right*, α, %).

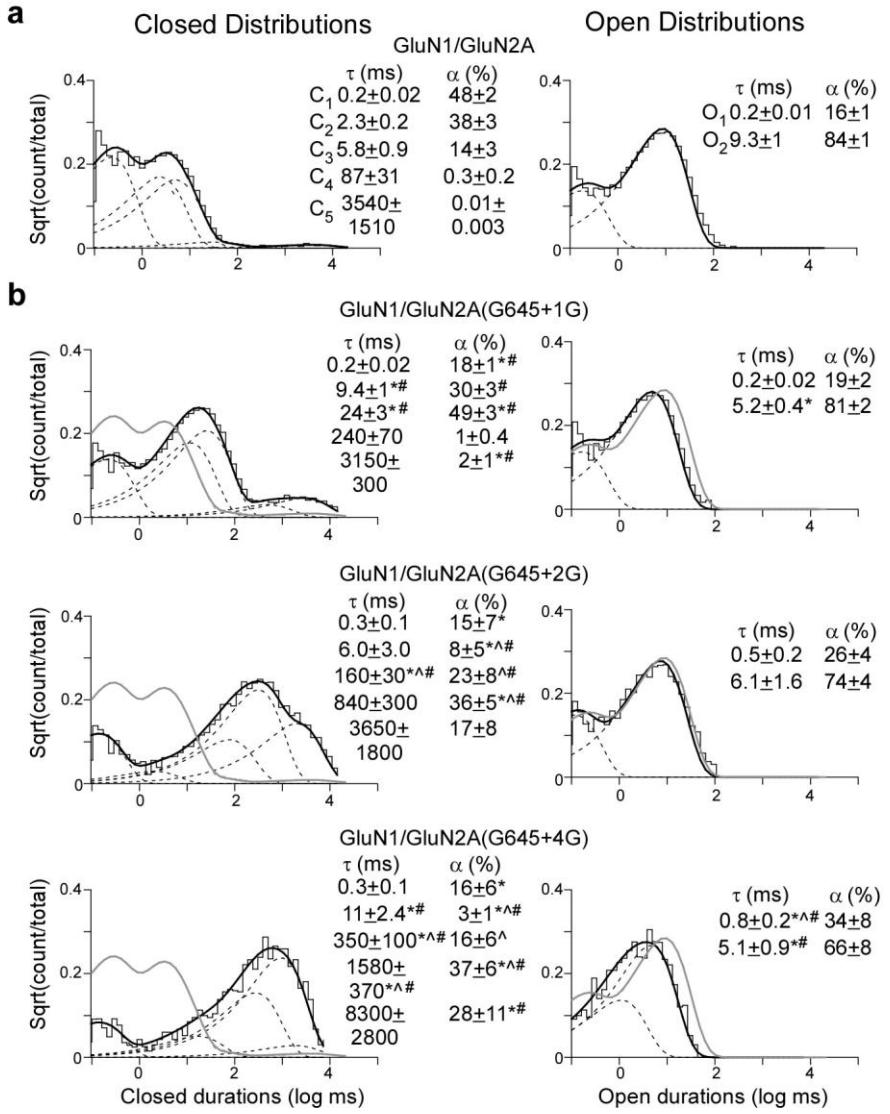

Supplementary Figure 6. Equilibrium open and closed time distributions for wild type and GluN2A insertion manipulations (relates to Fig. 6)
Figure is same as Supplementary Fig. 6 but for insertions in the GluN2A subunit.

Supplementary Table 4. Insertions alter activation kinetic rate constants (relates to Fig. 6)

		C_3–C_2	C_2–C_1	C_1–O_1	C_4–C_3	C_5–C_2	O_1–O_2
GluN1/ GluN2A	k_f	230±34	702±36	2930±340	0.5±0.1	35±14	3930±310
	k_r	37±7	2020±190	1210±150	4.5±1.1	2.3±0.9	570±47
	k_{eq}	7.1±0.8	0.4±0.03	2.6±0.3	0.1±0.04	15.9±3	7.1±0.7
	ΔG	–1.1±0.06	0.6±0.04	–0.5±0.07	1.3±0.2	–1.5± 0.2	–1.1±0.07
GluN1							
G648+1G	k_f	198±23	820±54	2090±270	0.4±0.05	36±11	3440±420
	k_r	32±3.7	2740±230*	1530±220	6.5±1.1	1.8±0.6	810±80*
	k_{eq}	6.5±0.8	0.3±0.03	1.4±0.2*	0.07±0.01	20.4± 5.0	4.5±0.6*
	ΔG	–1.1±0.06	0.7±0.05	–0.2±0.08*	1.6±0.09	–1.6± 0.2	–0.8±0.09*
G648+2G	k_f	170±24	1050±60*^	1440±280*	0.6±0.2	20±10	3940±580
	k_r	30±4.5	4420±320*^	2660±350*	6±1.1	1.1±0.3	1680±230*^
	k_{eq}	6±0.6	0.2±0.02*	0.5±0.09*^	0.07±0.01	14.0± 4.5	2.7±0.7*^
	ΔG	–1.0±0.06	0.8±0.06*	0.4±0.09*^	1.4±0.2	–1.4± 0.2	–0.5±0.2*
G648+4G	k_f	170±31	1030±25*^	1940±82*	0.4±0.06	22±12	4780±270^
	k_r	40±9.8	5380±360*^	3480±105*^	2.6±0.8^	2.0±0.9	1140±85*^
	k_{eq}	4.3±0.4*^	0.2±0.01*^	0.6±0.03*^	0.2±0.08	13.2± 3.6	4.2±0.2*
	ΔG	–0.8±0.06*^	1±0.03*^	0.3±0.03*^	1.1±0.3	–1.4± 0.2	–0.8±0.02*
GluN2A							
G645+1G	k_f	52±13*#	320±20*#	900±50*#	0.4±0.05	21±14	3590±370
	k_r	14.3±3*#	3170±300*	1440±230	6.1±1.4	4.6±3.6	830±67*
	k_{eq}	3.5±0.4*#	0.1±0.02*#	0.7±0.1*#	0.09±0.02	9.3±5.3	4.4±0.6*
	ΔG	–0.7±0.06*#	1.3±0.1*#	0.2±0.1*#	1.5±0.1	–1.0 ±0.2	–0.9±0.08*
G645+2G	k_f	93±45	140±40*^#	630±190*#	0.6±0.2	3.7±1.5	2400±1300
	k_r	210±87	4330±1420	1040±360#	0.8±0.3*^#	36±32	620±120#
	k_{eq}	0.6±0.2*^#	0.1±0.06*	0.8±0.3*	3.6±2.5	1.0± 0.5*#	3.9±1.8
	ΔG	0.5±0.3*^#	1.9±0.4*#	0.3±0.2*	–0.2± 0.4*^#	0.6±0.6*#	–0.4±0.4
G645+4G	k_f	34±8.0*#	36±7.7*^#	530±100*^#	0.4±0.1	3.3±1.4	1010±580*^#
	k_r	120±63	3800±980	750±210#^	0.4±0.2*^	6.4±3.9	570±100#
	k_{eq}	1.2±0.8*^#	0.01± 0.003*^#	1.0±0.3*	7.9±7.2	0.2± 0.04*#	1.5±0.6*^#
	ΔG	0.5±0.4*^#	2.7±0.2*^#	0.2±0.2*	–0.1± 0.4*#	1.4± 0.4*^#	0.1±0.3*^#

Mean values (± SEM) for forward (k_f) and reverse (k_r) equilibrium kinetic rate constants (s^{-1}) for a 5C–2O kinetic scheme (Fig. 6). ΔG is in units of kcal/mol. Kinetics models were constructed as C_3–C_2–C_1–O_1–O_2 while C_4 and C_5 branched from C_3 and C_2, respectively (see Online Methods). C_4 and C_5 reflect the desensitized states.